

# PCCP

Accepted Manuscript



This is an *Accepted Manuscript*, which has been through the Royal Society of Chemistry peer review process and has been accepted for publication.

*Accepted Manuscripts* are published online shortly after acceptance, before technical editing, formatting and proof reading. Using this free service, authors can make their results available to the community, in citable form, before we publish the edited article. We will replace this *Accepted Manuscript* with the edited and formatted *Advance Article* as soon as it is available.

You can find more information about *Accepted Manuscripts* in the [Information for Authors](#).

Please note that technical editing may introduce minor changes to the text and/or graphics, which may alter content. The journal's standard [Terms & Conditions](#) and the [Ethical guidelines](#) still apply. In no event shall the Royal Society of Chemistry be held responsible for any errors or omissions in this *Accepted Manuscript* or any consequences arising from the use of any information it contains.

## Structure-dependent water transport across nanopores of carbon nanotubes: toward selective gating upon temperature regulation

Cite this: DOI: 10.1039/x0xx00000x

Received 00th January 2012

Accepted 00th January 2012

DOI: 10.1039/x0xx00000x

www.rsc.org/

Kuiwen Zhao<sup>a</sup> and Huiying Wu<sup>a,\*</sup>

**Determining water structure in nanopores and its influence on water transport behaviour are of great importance for understanding and regulating the transport across nanopores. Here we report an ultrafast-slow flow transition phenomenon for water transport across nanopores of carbon nanotubes owing to the change of water structure in nanopores induced by temperature. By performing extensive molecular dynamics simulations, we show the dependence of water transport behaviours on water structures. Our results indicate that owing to the change of water structure in nanopores, water flux across nanopores with certain pore sizes decreases sharply (nearly 3 orders of magnitude) with the decreasing temperature. This phenomenon is very sensitive to the pore size. The threshold temperatures for the occurrence of the ultrafast-slow flow transition for water transport are also determined for various pore sizes. These findings suggest a novel protocol for selective gating of water and proton conduction across nanopores and temperature-controlled drug release.**

Transmembrane nanopores have intriguing applications to drug delivery<sup>1</sup>, molecular sieving<sup>2</sup>, single molecule detection<sup>3</sup>, water purification<sup>4</sup>, etc. They are also involved in many physiological processes and play an essential role in maintaining the homeostasis of living cells by regulating the transport of water, ions, and protons across membrane channels<sup>5</sup>. Water is a fundamental constituent for life and common medium for substance transportation. Water in nanopores shows complex structures and phase behaviors that differ greatly from those of bulk water<sup>6-9</sup>. Water structure (i.e. arrangement of water molecules) plays an important role in the substance transport process across nanopores<sup>10,11</sup>. Many transport processes across biological ion channels in cell membranes are controlled by the regulation of water structure<sup>10</sup>. Ionic and protonic conduction across nanopores, which is important in many natural phenomena including electrical signals communication in living systems, are also found to be influenced by water structure<sup>11</sup>. Water structure and its influence

on transport process inside nanopores have attracted increasing interests, however, previous work mainly focus on the water structure and transport behavior at constant room temperature<sup>6,12-15</sup>. The change of water structure with temperature and its influence on the water transport across nanopores is still unclear.

Here we report an ultrafast-slow flow transition phenomenon for water transport across nanopores owing to the change of water structure in nanopores induced by temperature. By performing extensive molecular dynamics simulations, we find that owing to the change of water structure in nanopores with the decreasing temperature, phase interfaces appear at the entrances of nanopores and thus the water flux across the nanopore decreases sharply (nearly 3 orders of magnitude). These findings suggest a novel protocol for selective gating of water and proton conduction across nanopores and temperature-controlled drug release.

Considering the pore size and temperature dependence of water structures, we perform molecular dynamics simulations of water transport across nanopores with a wide range of inner diameters (0.459-1.679 nm) over a large range of temperatures (253.15-373.15 K). To simplify the quantitative study, uncapped single-wall carbon nanotubes are chosen here as a simple model for nanopores. The inner channel of carbon nanotubes is well structured cylindrical shaped nanopore, the diameter of which can be tuned precisely by changing the chirality of nanotubes. The schematic illustration of the simulation system is shown in Figure 1a. The nanotube array separates two reservoirs of pure water. Water molecules transport across the inner channel of nanotubes. (All simulation details see Supporting Information.) Here, we define the water flux as the number of water molecules entering one nanotube from one side and leaving from the opposite side per nanosecond. In Figure 1b, we plot the water flux as a function of temperature for different pore sizes. It is shown that the variation in temperature has remarkably different effects on the water flux for different pore sizes. For the nanopores with inner diameters of 0.459, 1.001, and 1.679 nm, a 100 K decrease of temperature only causes a no more than 90% decrease of the water flux. Water maintains the ultrafast flow across the nanopores as the temperature decreases. The water flux obtained for the smallest pore size ( $d=0.459$  nm) is comparable to the rapid water flux measured through biological water channel aquaporin-1<sup>16,17</sup>, and also in the same magnitude to the

fast water flow across carbon nanotubes obtained in previous literature<sup>18</sup>. The small decrease of water flux with the decreasing temperature is ascribed to the decreasing self-diffusion coefficient  $D$  of bulk water, which exhibits the same decreasing feature as temperature decreases. In contrast, for the nanopores with inner diameters of 0.730, 0.798, and 0.905 nm, a 100 K decrease of temperature causes a more than 3 orders of magnitude decrease of the water flux. For the nanopores with inner diameters of 0.594 nm, the sharp decrease of water flux starts below 273.15 K.

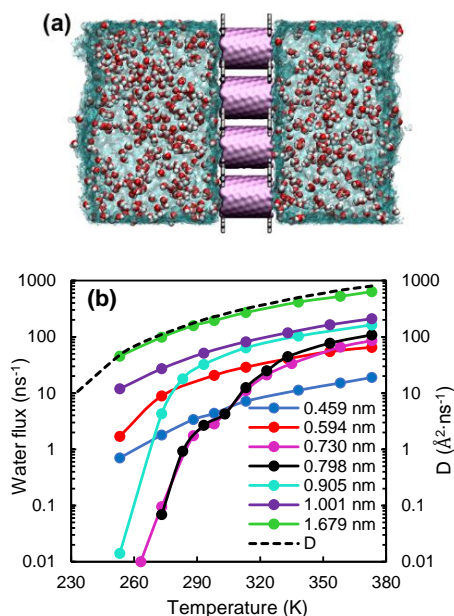


**Figure 1.** Properties of water transport across nanopores. (a) Schematic illustration of the simulation system for water transport across nanopores. Uncapped single-wall carbon nanotubes are selected as a simple model for nanopores. Nanotube array (purple tubes) separates two reservoirs of pure water. Water molecules transport across the inner channel of nanotubes. The channel length is 1.6 nm. For clarity, water molecules are selectively shown with red (O) and white (H) spheres. (b) Water flux versus temperature (253.15-373.15 K) for different pore inner diameters (0.459-1.679 nm). Also shown with the dashed line is the self-diffusion coefficient  $D$  of bulk water versus temperature.

The difference of water structure in nanopores plays a key role in above interesting water transport phenomena, which will be explained in detail below. Water molecules in nanopores with inner diameters of 0.459, 1.001 and 1.679 nm exhibit as free liquid molecules and no change of water structure with temperature is observed. Thus, water maintains the ultrafast flow as the temperature decreases. The same variation trend of water flux and self-diffusion coefficient  $D$  with temperature suggests that the self-diffusion of bulk water on two sides of nanopores contributes predominantly to the water transport process across nanopores. In contrast, water molecules in nanopores with inner diameters of 0.730, 0.798, and 0.905 nm exhibit square, pentagonal and hexagonal ordered ring-like structures, respectively, at relatively low temperatures (Figure 2a). Water molecules hydrogen bond with each other in the ring-like structure and stack together to form a solid-like highly ordered water structure (Figure 2b). Water within nanopores forms a different water phase from the bulk water and thus phase interfaces exist at the entrances of nanopores, which are barriers for water moving out of nanopores. Though the ordered water is highly diffusive inside the nanopore along axial direction<sup>14, 19</sup>, it is difficult for the water molecules in nanopores to penetrate the phase interfaces. When such ordered structure is broken at a higher temperature (Figure 2c), water molecules in nanopores behave as free

liquid molecules and thus no phase interface exists at the entrances of nanopores, making water molecules favorable to move out of the nanopores. Snapshots of simulations show that no strict temperature threshold exists for the appearance of ordered water structures. Take  $d = 0.798$  nm for example, even at a high temperature above 335 K, the ordered water structure still appears randomly in nanopores (Figure 2d and Supplementary Movie S1). But the appearance probability decreases dramatically with the increasing temperature. The relationship between the pore size and the change of water structure in nanopores with temperature will be discussed in detail later.

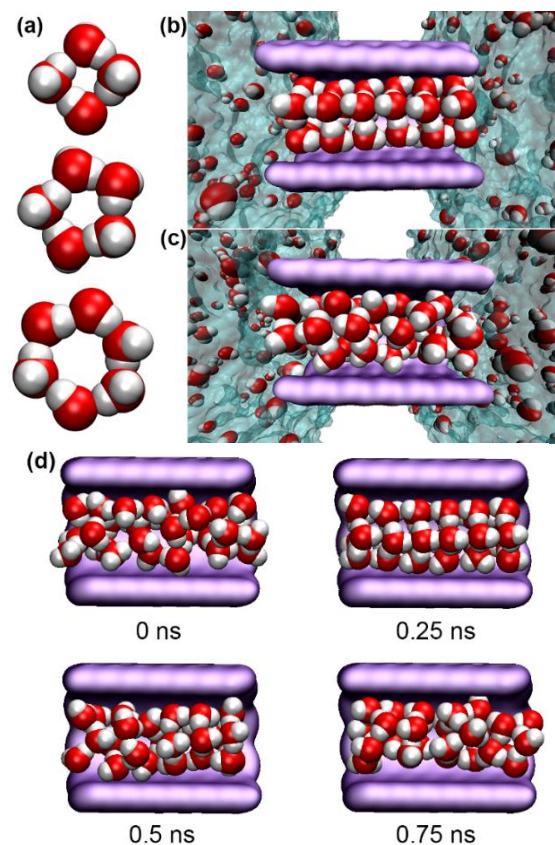


**Figure 2.** Water structures in nanopores. (a) Square, pentagonal, and hexagonal ring-like ordered water structures. (b, c) Snapshots of water structures in nanopores with inner diameter of 0.798 nm at 303.15 K (b) and 373.15 K (c). (d) Variation of water structure with time (snapshots of Supplementary Movie S1). Ordered water structure still appears randomly in the nanopore with inner diameter of 0.798 nm at 335 K.

To quantitatively identify the temperature-dependent water structure, we calculate the water orientation distribution at different temperatures for several pore sizes (Figure 3). Here the water orientation  $\theta$  is defined as the angle between the water molecular dipole vector and the nanotube axis. Remarkably, for  $d = 0.730$  and  $0.798$  nm, the orientation  $\theta$  of most water molecules at the temperature below 313.15 K mainly falls in the ranges of  $20^\circ$ - $60^\circ$  and  $120^\circ$ - $160^\circ$ , showing highly ordered structures. As the temperature increases above 335 K, the water orientation distributions tend to be uniform. The consistent change behavior of water structure with temperature for  $d = 0.730$  and  $0.798$  nm gives a satisfactory explanation for the observed similar water transport behavior in these two pore-sizes nanopores (Figure 1b). For  $d = 0.905$  nm, the appearance of highly ordered structures is observed below 283.15 K, 30 K lower than that for  $d = 0.730$  and  $0.798$  nm, matching well with the observed dozens

of kelvins delay in the abrupt decrease of water flux with the decreasing temperature (Figure 1b). In contrast, for  $d = 1.001$  nm, the water orientation distributions show no obvious change with

temperature. Similar phenomena with  $d = 1.001$  nm are also observed for  $d = 0.459$  and  $1.679$  nm, which well accounts for the similar water transport phenomena in these pore-sizes nanopores (Figure 1b).

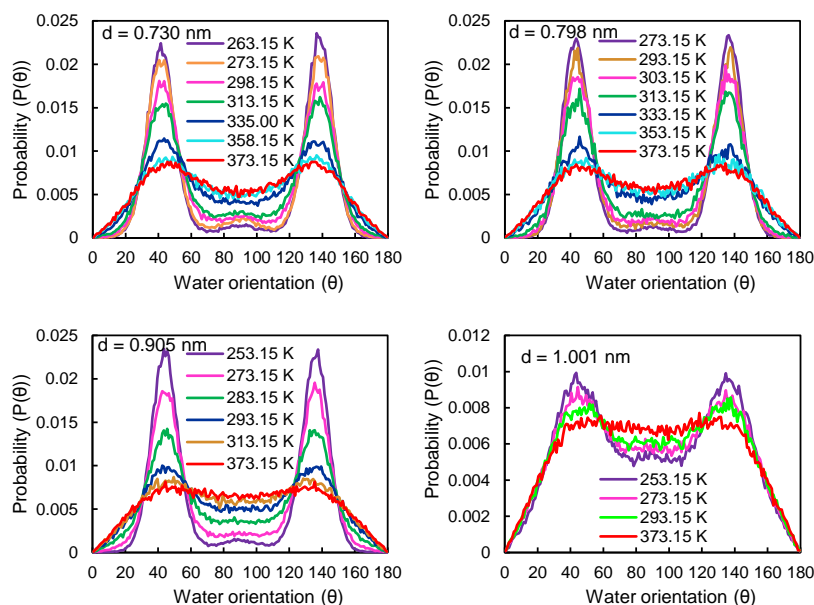


**Figure 3.** Water orientation distributions at different temperatures for inner diameter  $d = 0.730, 0.798, 0.905$  and  $1.001$  nm, respectively.

Considering the temperature-dependent water structure and its influence on water transport in nanopores, the determination of the threshold temperature below which all the water molecules in nanopores maintain ordered structures is helpful for the qualitative judgment of water transport behavior for different pore sizes. To solve this problem, we examine the instant mean water orientation and hydrogen-bond number of water molecules in a nanopore as a function of temperature for different pore sizes (Figure 4). Here we define a hydrogen bond as existing between two water molecules only when

their inner oxygen distance is less than  $3.5 \text{ \AA}$ , and simultaneously the O-H...O angle is less than  $30^\circ$ .<sup>20</sup> The water orientation and hydrogen-bond number versus temperature provide a clear identification of the transition between the ordered and disordered water structures. It is found that except for  $d = 1.001$  nm, both the mean water orientation and hydrogen-bond number for  $d = 0.730, 0.798,$  and  $0.905$  nm show a synchronous dramatic change, starting at the temperature of 317, 314, and 282 K, respectively. Snapshots of simulations show that all water molecules in nanopores below this temperature exhibit highly

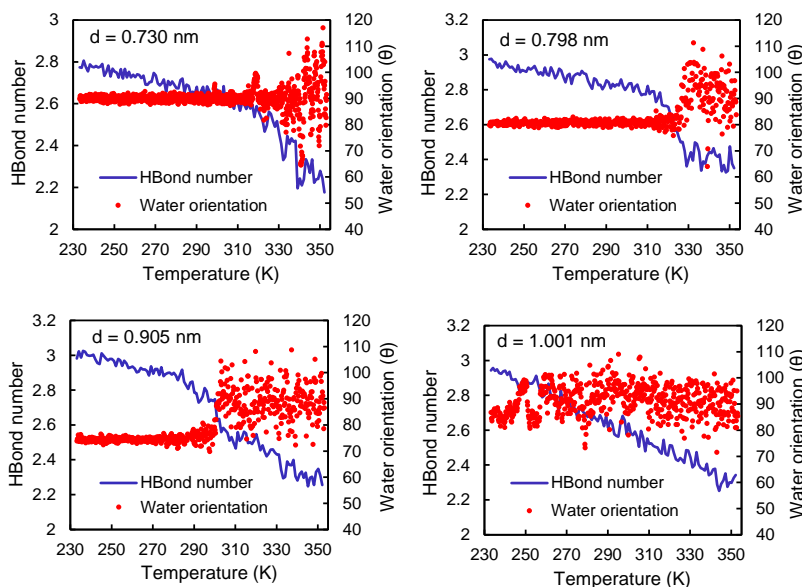


**Figure 4.** Mean water orientation and hydrogen-bond (HBond) number of water molecules in nanopores as a function of temperature (233-353 K) for inner diameter  $d = 0.730, 0.798, 0.905,$  and  $1.001$  nm.

ordered structures and no free liquid molecules are observed, thus it can be considered as the threshold temperature for fully ordered water in nanopores. We have obtained the threshold temperatures for  $d = 0.626\text{--}0.948$  nm with the above method (Figure 5). The water flux across nanopores decreases sharply as the temperature decreases close to the corresponding threshold temperatures (Figure 1b). Thus, the threshold temperature can be used to qualitatively predict the water structure-dependent ultrafast-slow flow transition for water transport across nanopores.

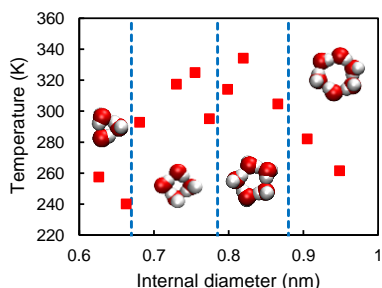


**Figure 5.** Threshold temperatures for fully ordered water in different-sized nanopores ( $d = 0.626\text{--}0.948$  nm). All the water molecules in nanopores maintain fully ordered structures below the threshold temperatures. Also shown are the ordered water structures appearing below the threshold temperatures.

Now let us discuss the physical mechanism for the formation of ordered water structures in nanopores at relatively high temperatures (i.e. temperatures above the freezing point of bulk water). Generally, hydrogen bonds are formed between water molecules by electrostatic attraction, which are unstable due to the stochastic thermal motion of water molecules. The stochastic thermal motion of water molecules in nanopores becomes weaker than that of bulk water due to the confinement of nanopores. Thus, the hydrogen bonds are more stable for water in nanopores, and then ordered water structures are formed at relatively high temperatures by the stable hydrogen bonding. The formation of certain ordered water structure (triangle, square, pentagon or hexagon) is dependent on whether the internal space of nanopores is big enough for the formation of water structures with more water molecules. It can be seen from Figure 5 that, even for the same water structure, the threshold temperatures for its formation are different for different pore sizes. Take pentagonal water structure formed in nanopores with  $d = 0.785\text{--}0.880$  nm for example, the highest threshold temperature is at  $d = 0.820$  nm. The threshold temperature decreases as the pore size becomes larger or smaller. This is because the stability of ordered water structures in nanopores is highly dependent on the competition between the hydrogen bonding and stochastic thermal motion of water molecules. The strength of hydrogen bonding between water molecules inside nanopores with  $d < 0.820$  nm is reduced by the stress exerted by nanopore walls. As the inner diameter increases to  $d > 0.820$  nm, though the space in nanopores is big enough to avoid the stress exerted on water structure, the stochastic thermal motion becomes stronger due to the enlargement of internal space of nanopores, which make the water structure unstable. Therefore, for both  $d < 0.820$  nm and  $d > 0.820$  nm, the ordered water structures becomes unstable, and thus the threshold temperature decreases.

As discussed above, water flows rapidly across nanopores when in the free disordered water state, while, as the temperature decrease to a threshold temperature, the water flux decreases sharply due to the appearance of ordered structures of water molecules in nanopores. The observed water flux under a pressure difference with ordered water structures in nanopores is even smaller than the prediction of

no-slip Hagen–Poiseuille equation (see Supporting Information). Generally, ordered water molecules form Grotthuss proton-conducting pathways<sup>21</sup> by hydrogen-bonding networks<sup>22</sup>, which is not effective for disordered water molecules (Figure 6). Therefore, our findings offer a protocol for selective gating the transport of water and proton across nanopores, which can be regulated by temperature. It is also worth noting that the water structures in nanopores are extremely sensitive to temperature. During the simulations, water molecules in nanopores always rearrange themselves rapidly within 0.06 ns to a favorable structure as the temperature changes, which means this temperature regulation method is highly sensitive. Considering the water structures in nanopores are highly dependent on the pore size of nanopores, the main challenge of this regulation method is to achieve nanopores with precise pore size. Currently, carbon nanotubes with diameters of 0.6–2 nm can be obtained via the control of nucleating nanoparticle size<sup>23</sup> and carbon feeding rate<sup>24</sup>, or other methods<sup>25,26</sup>. Besides, solid-state nanopores with diameters of 1–2 nm can be precisely fabricated via dielectric breakdown<sup>27</sup>. Further progress toward synthesizing nanopores with highly precise pore size will promote the practical feasibility of the regulation method proposed in this work.

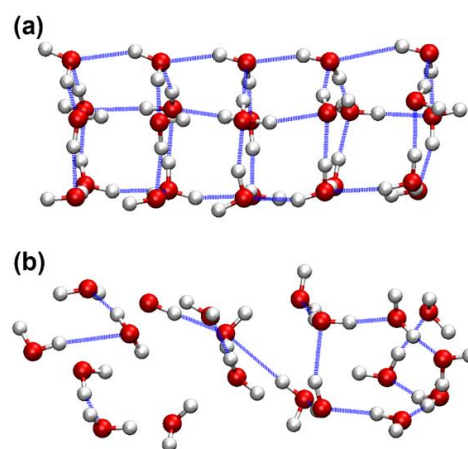


**Figure 6.** Hydrogen bonding of water molecules inside nanopores with inner diameter of 0.798 nm at 303.15 K (a) and 373.15 K (b). The blue dash lines represent hydrogen bonds. Hydrogen-bonding networks appear at 303.15 K due to the ordered water structure, which is broken at 373.15 K.

## Conclusions

We find an ultrafast-slow flow transition phenomenon induced by temperature for water transport across nanopores, which is attributed to the change of water structure in nanopores with temperature. The sharp decrease of water flux with the decreasing temperature, in combination with the appearance of highly ordered water structures, leads to a novel proposal for selective gating the transport of water and proton across nanopores. Besides, the water structure-dependent water transport behaviour demonstrated in this work is not only helpful for designing the effective nanoporous membranes for molecular sieving, water purification, and temperature-controlled drug release, but also helpful for deep understanding the regulation mechanism of transmembrane transportation in living cells.

## Acknowledgement

This paper was supported by the National Natural Science Foundation of China through grant nos. 51376130 and 50925624, National Basic Research Program of China (973 Program) through grant no. 2012CB720404, Science and Technology Commission of Shanghai Municipality through grant no. 12JC1405100.

## Notes and references

<sup>a</sup> School of Mechanical Engineering, Shanghai Jiao Tong University, Shanghai, 200240, China.

\*E-mail: whysrj@sjtu.edu.cn

Electronic Supplementary Information (ESI) available: [Methods, Comparison with continuum predictions, and Movie S1]. See DOI: 10.1039/c000000x/

1. G. Jeon, S. Y. Yang and J. K. Kim, *J. Mater. Chem.*, 2012, **22**, 14814-14834.
2. R. K. Joshi, P. Carbone, F. C. Wang, V. G. Kravets, Y. Su, I. V. Grigorieva, H. A. Wu, A. K. Geim and R. R. Nair, *Science*, 2014, **343**, 752-754.
3. M. Gershow and J. A. Golovchenko, *Nat. Nanotechnol.*, 2007, **2**, 775-779.
4. D. Cohen-Tanugi and J. C. Grossman, *Nano Lett.*, 2012, **12**, 3602-3608.
5. J. Liao, H. Li, W. Zeng, D. B. Sauer, R. Belmares and Y. Jiang, *Science*, 2012, **335**, 686-690.
6. P. Boynton and M. Di Ventra, *Phys. Rev. Lett.*, 2013, **111**, 216804.
7. K. Koga, G. T. Gao, H. Tanaka and X. C. Zeng, *Nature*, 2001, **412**, 802-805.
8. R. J. Mashl, S. Joseph, N. R. Aluru and E. Jakobsson, *Nano Lett.*, 2003, **3**, 589-592.
9. D. Takaiwa, I. Hatano, K. Koga and H. Tanaka, *Proc. Natl. Acad. Sci. U. S. A.*, 2008, **105**, 39-43.
10. J. Ostmeier, S. Chakrapani, A. C. Pan, E. Perozo and B. Roux, *Nature*, 2013, **501**, 121-124.
11. H. Dong, G. Fiorin, V. Carnevale, W. Treptow and M. L. Klein, *Proc. Natl. Acad. Sci. U. S. A.*, 2013, **110**, 17332-17337.
12. T. Ohba, *Angew. Chem. Int. Ed.*, 2014, **53**, 8032-8036.
13. A. Barati Farimani and N. R. Aluru, *J. Phys. Chem. B*, 2011, **115**, 12145-12149.
14. A. Striolo, *Nano Lett.*, 2006, **6**, 633-639.
15. A. Alexiadis and S. Kassinos, *Chem. Rev.*, 2008, **108**, 5014-5034.
16. M. L. Zeidel, S. V. Ambudkar, B. L. Smith and P. Agre, *Biochemistry*, 1992, **31**, 7436-7440.
17. B. L. de Groot and H. Grubmüller, *Science*, 2001, **294**, 2353-2357.
18. G. Hummer, J. C. Rasaiah and J. P. Noworyta, *Nature*, 2001, **414**, 188-190.
19. T. A. Pascal, W. A. Goddard and Y. Jung, *Proc. Natl. Acad. Sci. U. S. A.*, 2011, **108**, 11794-11798.
20. A. Luzar and D. Chandler, *Phys. Rev. Lett.*, 1996, **76**, 928-931.
21. S. Cukierman, *Biochim. Biophys. Acta-Bioenerg.*, 2006, **1757**, 876-885.
22. N. Agmon, *Chem. Phys. Lett.*, 1995, **244**, 456-462.
23. Y. Chen and J. Zhang, *Carbon*, 2011, **49**, 3316-3324.
24. C. Lu and J. Liu, *J. Phys. Chem. B*, 2006, **110**, 20254-20257.
25. T. Thurakitserree, C. Kramberger, P. Zhao, S. Chiashi, E. Einarsson and S. Maruyama, *Phys. Status Solidi B*, 2012, **249**, 2404-2407.
26. G. Chen, Y. Seki, H. Kimura, S. Sakurai, M. Yumura, K. Hata and D. N. Futaba, *Sci. Rep.*, 2014, **4**, 3804.
27. I. Yanagi, R. Akahori, T. Hatano and K.-i. Takeda, *Sci. Rep.*, 2014, **4**, 5000.